Nat. Hazards Earth Syst. Sci. Discuss., 1, 7701–7738, 2013
www.nat-hazards-earth-syst-sci-discuss.net/1/7701/2013/
doi:10.5194/nhessd-1-7701-2013

Natural Hazards and Earth System Sciences Discussions
Open Access

Future discharge drought across climate regions around the world modelled with a synthetic hydrological modelling approach forced by three General Circulation Models

N. Wanders[1] **and H. A. J. van Lanen**[2]

[1]Department of Physical Geography, Utrecht University, Utrecht, the Netherlands
[2]Hydrology and Quantitative Water Management Group, Wageningen University, Wageningen, the Netherlands

Received: 20 September 2013 – Accepted: 21 November 2013
– Published: 23 December 2013

Correspondence to: N. Wanders (n.wanders@uu.nl)

Published by Copernicus Publications on behalf of the European Geosciences Union.

Abstract

Hydrological droughts characteristics (drought in groundwater and streamflow) likely will change in the 21st century as a results of climate change. Magnitude and directionality of these changes and their dependency on climatology and catchment characteristics, however, is largely unknown. In this study a conceptual hydrological model was forced by downscaled and bias-corrected outcome from three General Circulation Models for the A2 emission scenario (GCM forced models), and the WATCH Forcing Data re-analysis dataset(reference model). The threshold level method was applied to investigate drought occurrence, duration and deficit volume. Results for the control period (1971–2000) show that the drought characteristics of each GCM forced model reasonably agree with the reference model for most of the climate types, suggesting that the climate model's results after post-processing produce realistic outcome for global drought analyses. For the near future (2021–2050) and far future (2071–2100) the GCM forced models show a decrease in drought occurrence for all major climates around the world and increase of both average drought duration and deficit volume of the remaining drought events. The largest decrease in hydrological drought occurrence is expected in cold (D-)climates where global warming results in a decreased length of the snow season and an increased precipitation. In the dry B-climates the smallest decrease in drought occurrence is expected to occur, which probably will lead to even more severe water scarcity. However, in the extreme climate regions (desert and polar), the analysis for the control period showed that projections are in these regions most uncertain. On a global scale the increase in hydrological drought duration and severity will lead to a higher impact of drought events, which urges water resources managers to timely anticipate on the increased risk on more severe drought in groundwater and streamflow and to design pro-active measures.

NHESSD
1, 7701–7738, 2013

1 Introduction

Droughts are caused by situations with less than normal natural water availability. They occur in all components of the hydrological cycle and occur across all climate regions throughout the globe (Wilhite, 2000; Tallaksen and Van Lanen, 2004; Mishra and Singh, 2010; Sheffield and Wood, 2011). On a global scale drought is one of the most severe natural hazards with large environmental and socio-economic impacts and more attention is require to be better prepared for the future water, food and energy security (Romm, 2011; Van Vliet et al., 2012). The recent summer droughts in Russia and Central US (National Oceanic and Atmospheric Administration, 2012) were the most severe on the record. The 2011 drought in the Horn of Africa caused large famine across Djibouti, Ethiopia, Kenya and Somalia (United Nations, 2011). In Europe almost 80 000 people died due to drought-related heat waves and forest fires, overall losses were estimated to be as high as 4940 billion Euro over the period 1998–2009 (EEA, 2010). Seneviratne et al. (2012) report that there is medium confidence that since the 1950s some regions of the world have experienced longer and more severe droughts (e.g. southern Europe and West Africa) and that droughts will intensify in the 21st century in some seasons and areas (e.g. many European regions, parts of North America, Central America, southern Africa) as result of climate change. Lack of long, updated time series of observed hydrological data (e.g. Hannah et al., 2011; Stahl et al., 2012), multiple definitions and drought-generating processes (e.g. Van Loon and Van Lanen, 2012), and the incapability of models to include all these processes (e.g. Gudmundsson et al., 2011; Haddeland et al., 2011; Prudhomme et al., 2011) impede our ability to instill strong confidence in the assessment of past and future drought across the world. High-impact large-scale droughts, like the recent droughts in Russia, the US, and Africa, show the need to improve understanding of droughts on continental and global scales, particularly to provide an improved assessment of climate change impact on drought.

Most global drought studies and near-real time drought monitoring programs focus on meteorological drought (in particular SPI, McKee et al., 1993), since meteorological data are widely available on a global scale. Other research has focused on soil moisture droughts on global scale (e.g. Dai et al., 2004; Sheffield and Wood, 2007; Sheffield et al., 2009; Dai, 2011; Orlowsky and Seneviratne, 2013). Global soil moisture droughts have been often examined (e.g. Dai et al., 2004; Dai, 2011) with the Palmer Drought Severity Index (PDSI, Palmer, 1965), which is calculated from a simple soil water balance, with the threshold method in combination with a more comprehensive model (e.g. Sheffield and Wood, 2007; Sheffield et al., 2009) or through anomalies (e.g. Orlowsky and Seneviratne, 2013). For water resources, it is particularly relevant how meteorological and soil moisture droughts propagate into hydrological drought (e.g. Peters et al., 2003; Tallaksen et al., 2009; Van Loon and Van Lanen, 2012). At large scales, Global Hydrological Models (GHMs) are used to produce runoff time series, which are then used for hydrological drought assessment. At the continental scale, Andreadis et al. (2005) investigated runoff drought in the United States and Prudhomme et al. (2011) studied European runoff drought. Forzieri et al. (2013) project for the A1B scenario and that future drought in streamflow will increase in many European regions, except for North and Northeast Europe. Corzo-Perez et al. (2011) and Van Huijgevoort et al. (2012) show hydrological drought characteristics at the global scale. These large-scale studies investigate which characteristics (frequency, scale, duration, severity) of past hydrological drought are captured with the GHGs to explore their potential to assess future continental and global drought. Recently, the WATCH (WATer and global CHange) project concluded a comprehensive multi-model analysis (e.g. Haddeland et al., 2011) that tested GHM performance against historic low runoff (e.g. Gudmundsson et al., 2011; Stahl et al., 2012) and drought (e.g. Prudhomme et al., 2011). Corzo-Perez et al. (2011) made a first attempt to use the outcome from the WATCH model suite to assess future hydrological drought across the globe (three General Circulation Models (GCMs), two scenarios, multiple hydrological models).

NHESSD
1, 7701–7738, 2013

N. Wanders and H. A. J. van Lanen

A detailed impact assessment on the importance of climate and catchment structure on drought occurrence is complicated since GHMs have a complex model structure with a large number of internal and external feedbacks mechanisms. To investigate the relative importance of climate and catchment structure on hydrological drought, Van Lanen et al. (2013) used a synthetic hydrological modelling approach to study the effects of these factors on hydrological drought characteristics on a global scale. The approach involved a conceptual hydrological model that was applied to a set of possible realizations of catchment characteristics (synthetic catchments) in combination with precipitation and evapotranspiration data from different climates around the globe. With this set-up Van Lanen et al. (2013) examined the relative importance of the physical catchment structure and meteorological forcing data (i.e. precipitation and evapotranspiration). They conclude that the physical catchments structure (i.e. the responsiveness of the groundwater system and soil type) has a similar impact on drought characteristics than climatology. However, the effects of climate change with respect to future hydrological drought across the world is largely unknown and difficult to study (Corzo-Perez et al., 2011).

The objective of this study is to examine the impact of climate change on hydrological drought at a global scale. Following the approach of Van Lanen et al. (2013) a synthetic hydrological model was used to model discharge time series at randomly selected locations in various climate regions around the world. Three GCMs provided model forcing data to the hydrological model and simulated droughts were compared against those derived from a reanalysis data (WATCH) forced model over the period 1971–2000 to explore uncertainty due to GCM forcing. Thereafter the effect of climate change was studied by the inter-comparison of modelled discharge time series and associated drought characteristics against the control period (1971–2000) for all GCM scenarios and the periods 2020–2050 and 2070–2100. The results allow a discussion on the projected impact of climate change on hydrological drought characteristics, including uncertainty, Which, in addition to impacts on meteorological and soil water drought characteristics, provide key information for planning of future water resources.

NHESSD
1, 7701–7738, 2013

2 Forcing data

2.1 WATCH Forcing Data

The WATCH Forcing Data (WFD) consist of time series of meteorological variables (e.g. rainfall, snowfall, temperature, wind speed) and are a product of the EU-FP6 project WATCH (WATer and global CHange). The WFD are derived from bias-corrected ECMWF ERA-40 reanalysis data (Uppala et al., 2005), which have a sub-daily, 1° resolution. For the WFD these data have been downscaled to 0.5° and temperature and specific humidity were bias corrected for elevation difference between the ERA-40 grid and WFD grid (Weedon et al., 2010, 2011). Another bias correction was applied to the daily temperature cycle and average temperature values using the CRU 2.0 data (Mitchell and Jones, 2005). Eventually a bias correction was applied to the number of "wet" days using the CRU data, while precipitation totals were corrected with the GPCCv4 dataset (Schneider et al., 2008). The CRU grid was used for the projection of the WFD resulting in a total of 67 420 land points at 0.5° × 0.5° resolution. The WFD for the period 1971–2000 have been used as a reference forcing dataset in this study. The WFD were used to identify the reference hydrological situation for every selected location, with the synthetic hydrological modelling approach.

2.2 General Circulation Models

In this study the output from three coupled atmosphere-ocean GCMs for the SRES A2 scenario (Nakićenović and Swart, 2000) has been used. Through the EU-WATCH project simulation outcome from three GCMS was available on a global scale and used for this study. The GCMs included are ECHAM5 (Roeckner et al., 2003; Jungclaus et al., 2006), CNRM3 (Royer et al., 2002; Salas-Mélia, 2002) and IPSL (Hourdin et al., 2006; Madec et al., 1998; Fichefet and Maqueda, 1997; Goosse and Fichefet, 1999). Additional GCMs simulation from other projects were not used since these used other bias correction approaches and data than the three GCMs selected for this study. Each GCM provides meteorological forcing for the period 1960–2100. We used the period 1971–2000 as control period. The same procedure as for the WFD was applied in WATCH to downscale each GCM to the higher resolution 0.5° grid of the WFD. The WFD were used to determine the bias correction required for rainfall, snowfall, minimum, mean and maximum air temperature for the control period. The procedure is described in more detail by Piani et al. (2010a), Piani et al. (2010b), Chen et al. (2011), Haerter et al. (2011). Detailed information on the GCMs can be found in Table 1. The data from the GCMs were used as meteorological input data for the synthetic hydrological modelling approach to produce discharge time series and associated drought characteristics for: (i) the control period (1971–2000), and (ii) the periods 2021–2050 and 2071–2100 to intercompare obtained drought characteristics against those derived from the reference model (1971–2000).

3 Model framework

3.1 Model description

The synthetic hydrological model, is a lumped conceptual hydrological model, which consists of reservoirs for snow cover, soil moisture and groundwater (Fig. 1). The model concept is a simplified representation of the natural system that simulates daily fluxes and state variables. The synthetic hydrological model generates time series of potential realizations for soil moisture storage and groundwater discharge without use of specific local catchment information apart from meteorological forcing (synthetic catchments). The simulations do not claim to provide actual site specific soil moisture storage and groundwater discharge, but rather give a possible realization of these variables given the local meteorological data. The water balance of the modelled soil moisture is given by:

$$SS(t) = SS(t-1) + P_{rain}(t) + Q_{snow}(t) - E_{act}(t) - Q_s(t) \quad (1)$$

NHESSD
1, 7701–7738, 2013

where, SS is the soil moisture storage (mm), P_{rain} the rainfall ($\mathrm{mm\,d^{-1}}$), Q_{snow} the snow melt ($\mathrm{mm\,d^{-1}}$), E_{act} the actual evapotranspiration ($\mathrm{mm\,d^{-1}}$) and $Q_{\mathrm{s}}t$ is recharge generated by percolation through the unsaturated zone ($\mathrm{mm\,d^{-1}}$). The model is forced with daily temperature, precipitation and potential evapotranspiration to enable snow accumulation, soil moisture, actual evapotranspiration and discharge simulations. Estimates of daily evapotranspiration was calculated using the Penman-Monteith reference evapotranspiration (McMahon et al., 2013). The potential evapotranspiration was calculated from daily temperature (minimum, mean, maximum), air pressure and wind speed (Allen et al., 2006). The daily mean temperature was also used in the snow-module for snow accumulation and melt, following the widely-accepted approach of the HBV-model (Seibert, 2002). Precipitation is simulated as snow when air temperature is below a pre-defined threshold, snow melt only occurs above the threshold temperature and is simulated with the degree-days approach (Clyde, 1931; Collins, 1934). The snow water balance of the snow module is given by:

$$\mathrm{Sn}(t) = \mathrm{Sn}(t-1) + P_{\mathrm{snow}}(t) - Q_{\mathrm{snow}}(t) \tag{2}$$

where Sn is the snow storage (mm) and P_{snow} is snowfall ($\mathrm{mm\,d^{-1}}$). The groundwater recharge ($\mathrm{mm\,d^{-1}}$) is given by:

$$Q_{\mathrm{rch}}(t) = Q_{\mathrm{s}}(t) + Q_{\mathrm{b}}(t) \tag{3}$$

where $Q_{\mathrm{b}}(t)$ is recharge generated by bypass in the unsaturated zone ($\mathrm{mm\,d^{-1}}$). The percolation through the unsaturated zone is given by:

$$\begin{array}{ll} Q_{\mathrm{s}}(t) = \mathrm{SS}(t) - \mathrm{SS_{FC}} & \text{if } \mathrm{SS}(t) \geq \mathrm{SS_{FC}} \\ Q_{\mathrm{s}}(t) = \left(\frac{\mathrm{SS}(t)-\mathrm{SS_{CR}}}{\mathrm{SS_{FC}}-\mathrm{SS_{CR}}}\right)^{b} k_{\mathrm{FC}} & \text{if } \mathrm{SS_{CR}} \leq \mathrm{SS}(t) \leq \mathrm{SS_{FC}} \\ Q_{\mathrm{s}}(t) = 0 & \text{if } \mathrm{SS}(t) \leq \mathrm{SS_{CR}} \end{array} \tag{4}$$

where SS(t) (mm) is the soil moisture content at time t (d), b is a shape parameter derived from the soil retention curve (–), k_{FC} is the unsaturated hydraulic conductivity at field capacity (mm d^{-1}), SS_{CR} and SS_{FC} (mm) are the critical and field capacity soil moisture content, respectively. The bypass to the groundwater ($Q_b(t)$) is 50 % of the rainfall above 2 mm, when the soil is below SS_{CR} to simulate flow through the macropores of the unsaturated zone. A soil with an intermediate soil moisture supply capacity was selected to simulate the response of the unsaturated zone (Van Lanen et al., 2013). This soil has a total supply capacity of 125 mm where about 75 mm is readily available for evapotranspiration. The water balance of the groundwater system is given by:

$$\mathrm{GS}(t) = \mathrm{GS}(t-1) + Q_{\mathrm{rch}}(t) - Q_{\mathrm{dis}}(t) \tag{5}$$

where GS is the groundwater storage (mm) and Q_{dis} is the groundwater discharge (mm d^{-1}). The Q_{dis} is calculated with the De Zeeuw–Hellinga approach (Kraijenhof van de Leur, 1962; Ritzema, 1994):

$$Q_{\mathrm{dis}}(t) = Q_{\mathrm{dis}}(t-1) \cdot e^{\frac{-1}{j}} + Q_{\mathrm{rch}}(t) \cdot (1 - e^{\frac{-1}{j}}) \tag{6}$$

where j is the groundwater response parameter (d), which can be derived from data on the aquifer transmissivity, storativity and the distance between rivers. The j value in this study was fixed to 250 d, which corresponds to an intermediate-responding groundwater system. The groundwater discharge is hereafter called discharge ($Q = Q_{\mathrm{dis}}$). The ability of the synthetic model to reproduce observed streamflow was demonstrated by Tijdeman et al. (2012). For a more detailed description of the synthetic hydrological modelling approach the reader is referred to Van Lanen et al. (2013).

3.2 Drought identification

Hydrological drought characteristics (e.g. drought duration and deficit volume) were derived from simulated time series of daily discharge (Q) using the threshold level approach (Yevjevich, 1967; Tallaksen et al., 1997; Hisdal et al., 2004). In this study the

Q_{80} (mm d^{-1}) was derived from the flow duration curve, where the Q_{80} is the threshold which is equalled or exceeded for 80 % of the time. The Q_{80} has been used in multiple studies where drought is studied (e.g Fleig et al., 2006; Parry et al., 2010). A monthly threshold was applied, where the Q_{80} is derived for every month of the year. With a moving average window of 30 days the threshold was smoothed, resulting in the variable monthly threshold used for this study (Van Loon and Van Lanen, 2012). The drought state is given by:

$$\begin{aligned} \mathrm{Ds}(t) = 1 \quad & \text{for} \quad Q(t) < Q_{80}(t) \\ 0 \quad & \text{for} \quad Q(T) \geq Q_{80}(t) \end{aligned} \tag{7}$$

where $\mathrm{Ds}(t)$ is a binary variable indicating if a location is in drought at time t. The drought duration for each event was calculated with:

$$\mathrm{Dur}_i = \sum_{t=S_i}^{L_i} \mathrm{Ds}(t) \tag{8}$$

where Dur_i is the drought duration (d) of event i, S_i the first time step of a event i and L_i the last time step of the event. The Percentage Drought per Year (PDY) was used in this study as a measure of drought occurrence that enables a comparison between the simulated discharge time series of different time periods (e.g. 2021–2050 relative to 1971–2000). The PDY was calculated by:

$$\mathrm{PDY} = \frac{\sum_{t=1}^{Y \cdot 365} \mathrm{Ds}(t)}{Y} \tag{9}$$

where PDY is the fraction of the total simulation period that a location is in drought (d yr^{-1}) and Y is the number of years. Please note that PDY = 73 d yr^{-1} for the control

NHESSD
1, 7701–7738, 2013

Future discharge drought

N. Wanders and H. A. J. van Lanen

period 1971–2000 by definition. The deficit volume was defined by:

$$\mathrm{Def}(t) = \begin{cases} Q_{80}(t) - Q(t) & \text{for } \mathrm{Ds}(t) = 1 \\ 0 & \text{for } \mathrm{Ds}(t) = 0 \end{cases} \tag{10}$$

where $\mathrm{Def}(t)$ is the daily deficit volume of drought i (mm). The total drought deficit volume for each drought event was calculated with:

$$\mathrm{Def}_i = \sum_{t=S_i}^{L_i} \mathrm{Def}(t) \tag{11}$$

where Def_i is the total deficit volume of the drought event i (mm). The deficit volume is the cumulative deviation of the discharge from the threshold over the duration of a drought event. Furthermore, the standardized deficit volume (d) was obtained with:

$$\mathrm{StDef}_i = \frac{\mathrm{Def}_i}{\overline{Q}} \tag{12}$$

where StDef_i is the deficit volume of event i (d^{-1}) divided by $\overline{Q}$, the mean yearly discharge ($\mathrm{mm\,d^{-1}}$). StDef_i was introduced to enable a comparison across the globe between locations with different flow magnitudes. Since the deficit volume (Def_i) is highly correlated to the discharge, the obtained StDef provides the drought severity relative to the local hydrological situation. The drought duration and standardized deficit volume are hereafter referred to as the duration and deficit volume. If the Q_{80} equals $0\,\mathrm{mm\,d^{-1}}$ for more than 20 % of the time, no drought characteristics were calculated since by definition a drought will not occur (Eq. 7). These locations were excluded from the analysis, since frequent zero discharge situations are part of the local climate (i.e. aridity) and are not a situation with below normal water availability. When a drought is already present at the beginning of a simulation period or still present at the end no valid characteristics could be obtained and therefore the drought event was excluded from the analysis to avoid including incomplete drought events in the statistics.

NHESSD
1, 7701–7738, 2013

3.3 Similarity Index

The Similarity Index (SI) was introduced as a measure to examine changes in drought characteristics (Van Lanen et al., 2013). Bivariate probability distributions (Wand and Jones, 1995) were used to find relations between drought duration (Eq. 8) and deficit volume (Eq. 12). The bivariate probability distributions were compared for different scenarios (e.g different time periods) and their joint occurrence was evaluated with the SI. The area of the 90 % of the bivariate probability distribution field was calculated and used for further evaluation. Both low and high extreme values of Dur_i and Def_i were excluded, since the focus of this study is on changes in the most extreme drought conditions. The Similarity Index (SI) quantifies the degree of overlap (%) between two 90 % Dur – StDef probability fields as follows:

$$
\begin{aligned}
&\mathrm{SI} = \frac{R1|R2}{R1} \cdot 100 \\
&R1 = \sum_{x=1}^{m} \sum_{Y=1}^{n} \mathrm{MR1}(m,n) \qquad \text{if } \mathrm{MR1}(m,n) = 1 \\
&R1|R2 = \sum_{x=1}^{m} \sum_{Y=1}^{n} \mathrm{MR1}(m,n) \text{ if } \mathrm{MR1}(m,n) = 1 \text{ and } \mathrm{MR2}(m,n) = 1
\end{aligned}
\tag{13}
$$

where $R1$ is the 90 % Dur–StDef probability field of realization of scenario 1, $R1|R2$ is the coinciding 90 % Dur–StDef probability fields of realizations of scenarios 1 and 2 (e.g. 1971–2000 and 2021–2050, respectively). MR1 and MR2 are matrices, MR1 contains the conditional probabilities of realization of scenario 1, and MR2 the field of realization of scenario 2. $\mathrm{MR1}(m,n)$ and $\mathrm{MR2}(m,n)$ are binary quantities where 1 equals a value within, and 0 a value outside the 90 % Dur–StDef probability field of realizations 1 and 2, respectively. In this study $m \cdot n$ was set at $150 \cdot 150$ and physical limits of Dur and StDef where fixed to 1296 (d) and 256 (d), respectively. By definition the SI can range between 0 % (no joint occurrence) and 100 % (complete joint occurrence). For a more detailed description of the SI the reader is referred to Van Lanen et al. (2013).

NHESSD

1, 7701–7738, 2013

Future discharge drought

N. Wanders and H. A. J. van Lanen

3.4 Selection of evaluation locations

For a global evaluation of the change in drought duration and deficit volume as result of climate change, locations (i.e. WATCH cells) were randomly selected around the world. The Köppen–Geiger climate classification (Köppen, 1900; Geiger, 1954, 1961) was used to ensure that locations were selected in all different major climate regions. The five climate types distinguished in this study are: Equatorial (A), Arid (B), Warm temperate (C), Snow (D) and Polar climates (E). The global map with Köppen–Geiger climate classification was recalculated based on the WFD, to obtain correct positioning of climate regions (Wanders et al., 2010). The 1495 locations identified by Van Lanen et al. (2013) were also used for this study. They show that at least 30 randomly selected locations are required per major climate region to obtain reliable general drought characteristics. The selected locations were distributed over the climate types A, B, C, D and E as follows: 16, 21, 16, 34, and 13 %, which reflect differences in area of major climate regions.

3.5 Impact assessment of climate change

To examine the impact of climate change on characteristics of discharge droughts, the synthetic hydrological modelling approach was used and forced with meteorological data from three GCMs (GCM forced) over the period 1960–2100. This period was divided into three evaluation periods, namely 1971–2000, 2021–2050, 2071–2100. An eleven year warm-up period (1960–1970) was applied for the hydrological model to remove biases resulting from the initial conditions. The monthly Q_{80} was derived over the period 1971–2000 to determine the variable threshold (Sect. 33.2). The 1971–2000 threshold was applied to the two other future periods, to enable calculation of the drought characteristics (D and StDef, Eqs. 8 and 12) and to determine the effect of climate change relative to the period 1971–2000. The effect of climate changes on drought duration and deficit volume was studied for all different major climate regions. The discharge drought characteristics of each GCM forced hydrological model over the

NHESSD
1, 7701–7738, 2013

control period (1971–2000) were compared against the characteristics derived from the model forced with the WFD for the same period (reference model) to explore uncertainty due to GCM forcing. Ideally, there should be only minor differences in drought characteristics between the characteristics derived from discharge simulated with the GCM forcing and the simulation with the WFD, since the control periods of each GCM are bias corrected to match the WFD (Piani et al., 2010a, b; Haerter et al., 2011; Chen et al., 2011; Hagemann et al., 2011). The changes in drought characteristics were evaluated for the period 2021–2050 and 2071–2100 by comparing against the control period of each GCM forced hydrological model. For the evaluation the SI was calculated for all major climate types and used to determine the changes in drought duration and deficit volume as a result of a changing climate.

4 Results

4.1 Control period

Hydrological droughts derived from discharge time series that were simulated with the synthetic hydrological modelling approach using re-analysis data (WFD) as meteorological forcing (reference model) were benchmark in this study. The hydrological drought characteristics were intercompared for the control period from 1971–2000 with those obtained from the same hydrological model that was forced with downscaled and bias-corrected outcome from three GCM forced models.

The bivariate density distributions obtained for the control period for all three GCM forced models show large similarity with the reference model for all climate types (Fig. 2). However, some deviations occur for the polar (E) and arid (B) climate types where the GCM force models show less spread in the drought characteristics than the reference model. Overall the GCM forced models show a large resemblance to the reference model throughout the climate regions, especially for the less extreme climate

NHESSD
1, 7701–7738, 2013

Title Page
Abstract | Introduction
Conclusions | References
Tables | Figures
◀| |▶
◀ ▶
Back | Close
Full Screen / Esc
Printer-friendly Version
Interactive Discussion

types. This is also illustrated through the Similarity Index (SI, Eq. 13) when the GCM forced models are compared against the reference model (Table 2).

The average drought duration and deficit volume for the major climates and averaged over all climates show that the GCM forced models are in good agreement with the reference model with some mismatch in the extreme arid and polar climate types. The results from Table 3 support the SI findings (Fig. 2 and Table 2), that the GCMs are capable to produce realistic meteorological forcing for hydrological drought assessment under most climate conditions, but show difficulties in desert and polar climates. The drought duration derived from the GCM forced models for the A, C and D major climate types deviates less than 10 % from the duration obtained for the reference model (Table 2, IPSL for the A climate type is an exception). For the B and E climates the deviation is larger in particular for the latter (up to more than 50 %). The deficit volume shows a similar pattern but relative deviations are larger because of smaller magnitude (Table 2).

4.2 Future period

All GCM forced models show a decrease in the number of hydrological droughts throughout climate types (Fig. 3, upper row, note logarithmic scale). This decreasing number of droughts is associated with an increase in the duration by 143–157 % for all GCM forced models in 2071–2100 (Fig. 3, second row, Table 4). The most severe droughts also show a very strong increase relative to the control period and the spread in duration between locations strongly increases. The overall effect of climate change on the PDY over the two future periods shows a decreasing trend (Fig. 3, third row). The total time a location is in drought decreases by 67–74 % in 2071–2100 (Table 4), indicating that the locations are less in drought throughout the 30 yr period. The deficit volume shows an overall increase of slightly over 200 % in 2071–2100 (Table 4), which indicates that although droughts are less frequent, the severity in both duration and deficit volume increases.

NHESSD
1, 7701–7738, 2013

Future discharge drought

N. Wanders and H. A. J. van Lanen

The projected changes in the median of discharge drought characteristics (duration, deficit volume and PDY) for each major climate type are included in Table 4. The duration increases relative to the control period in all major climate regions, where the period 2071–2100 is more affected than 2021–2050 (Table 4). The strongest increase occurs for the equatorial and arid climates, where duration increases up to 181 % for IPSL. For the snow and polar climate (D, E) the increase in duration is smaller (114–138 %) and lower than for the warmer A, B and C climates.

The PDY is projected to decrease throughout the 21st century. However, changes vary throughout climate regions. Averaged over all climates by the end of the century, median PDY will decrease to 26–33 % relative to the control period leading to an average of $\approx 22\,\mathrm{d\,yr^{-1}}$. For the equatorial climate (A) the direction of the change is not uniform. The IPSL forced model shows an increase for the equatorial climate (A) in 2071–2100, while both ECHAM and CNRM show that the PDY will decrease throughout all climate types. For the other climate regions the direction of the change is uniform and shows a decrease in the PDY. For the snow climate, the changes are largest, the total PDY reduces to 5–8 % relative to the control period, leading to an average PDY of $\approx 5\,\mathrm{d\,yr^{-1}}$ by the end of the 21st century.

A substantial increase was found for the deficit volume for all climate regions in both future periods, where the median deficit volume clearly increases over the century. This increase is strongest for the A, B and C climates, where the ranges increase by 217–327 % leading to median deficit volumes between 9.24 and 21.6 d, i.e. 9.24 and 21.6 times the mean discharge.

For all future GCM forced models the 90 % probability fields were calculated and the changes relative to the control period are presented using the SI (Table 5). All models indicate that changes occur with a similar magnitude for all major climate types. For example, the SIs obtained with the ECHAM forced model show that 19 % of drought characteristics (duration and deficit volume) of events in 2021–2050 (averaged over all climates), did not occur in the control period. This percentage increases up to 31 % by the end of the century. The strongest decrease in SI (i.e. largest change) was found in the equatorial, arid and warm temperate climates (A, B, C) where SI values can be as low as 60 %. The same pattern was found for the snow climate (D), however, changes in SI are smaller.

5 Discussion

Most global drought projections address meteorological or soil moisture drought. Dai (2012) has investigated global soil moisture drought up to 2010 and states that the PDSI changes derived from observed weather records are consistent with model predictions, which would indicate severe and extended global droughts in the 21st century resulting from either decreased precipitation and/or increased evaporation. Sheffield et al. (2012) argue that the increase in global soil moisture drought since the 1980s is overestimated because the PDSI is a too simplified model, which has consequences of how to interpret the impact global warming on global drought changes. Orlowsky and Seneviratne (2013) use meterological drought (SPI) and soil moisture drought (anomaly) to illustrate that there will be both wetting regions in the 21st century (e.g. East and South Asia, Sahel, Central North America, Central Europe) and drying regions (e.g. Australia, South Africa, Central America, Amazon, Mediterranean). Seneviratne et al. (2012) conclude that there is medium confidence that in some regions across the world duration and intensity of meteorological or soil moisture drought will increase and elsewhere the confidence level is low because of definitional differences or model disagreement. Land surface processes and properties (e.g. groundwater flow and storage, stream–aquifer interaction, (Van Lanen et al., 2004; Van Loon et al., 2012) make meteorological or soil moisture drought projections not straightforwardly applicable to hydrological droughts.

Hydrological drought projections, which are of paramount importance for assessments of future water resources, are still limited. GCMs and Regional Climate Models (RCMs) are somewhat simplified to include all relevant land surface processes and properties, hence usually lack adequate soil and aquifer storage processes (Stahl et al., 2011). Drought projections are often associated with change in annual runoff or river flow (e.g Arnell, 2003; Milly et al., 2005). Off-line approaches on a global scale use large-scale hydrological models in combination with forcing from either GCMs or RCMs. Intermediate approaches are needed to downscale and bias correct the climate model forcing (Haddeland et al., 2011), which is a challenging process (e.g Sperna Weiland et al., 2010; Hagemann et al., 2011), in particular for the future climate (Chen et al., 2011). Very few attempts have been made so far to derive hydrological drought characteristics at the global or continental scale under future climate. Forzieri et al. (2013) project an increase in deficit volume of river flow for vast areas of Europe, except the Scandinavian countries and North Russia. Hirabayashi et al. (2008) and Feyen and Dankers (2009) project a substantial increase in the number of drought days (PDY) or flow deficit volume for the period 2071–2100 in some regions, whereas in contrast, wide areas will benefit from a decrease in drought days. An increase in number of drought days in general is not in line with the modelling experiment in this study, whereas an increase in deficit volume is supported (Table 4). Corzo-Perez et al. (2011) analysed future drought for two time domains (2021–2050 and 2071–2100), two emission scenarios (A2 and B1), 3 downscaled and bias-corrected GCMs, and 5 large-scale hydrological models. The number and spatial distribution of drought events did not clearly show a consistent change. The limited number of global studies on future hydrological drought still make projections uncertain.

In the control period 1971–2000, differences occur between hydrological drought characteristics (Fig. 2) derived from discharge time series simulated with meteorological forcing from downscaled and bias-corrected outcome from three Global Circulation Models (GCM forced models). For example, the duration and deficit volume averaged over all climates varies from 60 to 69 d and from 5.05 to 5.94 d, respectively, for the three GCM forced models (Table 3). The mean reason for this are the GCM model structures (Chen et al., 2011; Haerter et al., 2011). Differences in hydrological drought characteristics among GCM forced models are more similar than the differences between characteristics derived form the GCM forced models and

NHESSD
1, 7701–7738, 2013

characteristics that were obtained using re-analysis data as meteorological forcing (reference model) as meteorological forcing. Exceptions are the B and E climates (Tables 2 and 3). For the A, C and D climates differences in drought duration of GCM forced models against the reference model vary from 0 to 30 %, whereas for the deficit volume the range is 1–26 %. Differences in drought characteristics between GCM forced models and the reference model are mostly negative implying that the drought duration and standard deficit volume are smaller when GCM forcing was used instead of re-analysis data. Differences in drought characteristics against the reference model are not always mono-directional for a particular climate (e.g. drought duration for the C climate). The above-mentioned differences are a measure for climate model uncertainty. Most large-scale studies, which explore hydrological impact of climate change, compare simulated and observed annual river flow to assess model fitness as a basis for projections (e.g Arnell, 2003; Milly et al., 2005). Other studies also focus on low-water availability and include minimum flow or flow deficits to investigate future drought (e.g Feyen and Dankers, 2009; Forzieri et al., 2013). Few large-scale studies test hydrological model performance by comparing GCM forcing against observed forcing. Sperna Weiland et al. (2010) are such an exception. They conclude that bias-corrected GCM-forcing should be used with caution for global hydrological impact studies in which persistence is relevant, like for drought. Another example is Corzo-Perez et al. (2011), who confirm that for a control period no clear patterns can be found in differences between hydrological drought characteristics derived from GCM-forced hydrological models and the same models forced with re-analysis data.

Global annual precipitation totals is projected to increase throughout the 21st century, although locally annual precipitation might decrease (Solomon et al., 2007). Precipitation increase is most prominent in the equatorial and polar climates, resulting in an increase in discharge (Solomon et al., 2007), which was confirmed by the data from GCMs that we used for this study. Therefore, in the 21st century the historic Q_{80} (1971–2000) was exceeded for more than 80 % of the time in our study, hence the PDY decreased both in the near and far future (Table 4).

It was noticed that for the equatorial climate the impact of climate change is not unambiguous. Two GCM forced models (ECHAM, CNRM) indicate a decrease in total drought occurrence (PDY) relative to the control period (19–25 % for 2012–2050 and 36–56 % for 2071–2100), while one GCM forced model (IPSL) indicates a small increase (12 % for 2012–2050 and 28 % for 2071–2100) in total drought occurrence (A climate, Table 4). The main reason for the model disagreement is an increase in precipitation projected by ECHAM and CNRM and a decrease by IPSL in most of the selected locations for the A climate leading to higher and lower discharge, respectively.

The three GCMs project increasing annual temperatures leading to a decreased length of the snow accumulation period in cold climates (D- and E-climates), which have great impact on river flow (e.g Wilson et al., 2010), and consequently on drought occurrence (PDY, D climates, Table 4). For instance, duration of rain-to-snow-season droughts as identified by Van Loon and Van Lanen (2012) will decrease due to later precipitation as rain in autumn or earlier rain in spring leading to quicker snow melt peak. It was found that the combined effect of increased precipitation and shorter snow accumulation periods causes a strong decrease in total drought duration (i.e. PDY). Feyen and Dankers (2009) report on a decrease in drought severity (i.e. 7 day minimum flow and deficit volume during the frost period) in the cold European climates. Classical rainfall droughts, however, will become more severe due to lower summer flows in some regions, e.g. southern and eastern Norway (Feyen and Dankers, 2009; Wilson et al., 2010; Wong et al., 2011; Stahl et al., 2011), which is supported by this study, where the remaining drought in the far future last 14–29 % longer and are 26–52 % more severe.

6 Conclusions

With a synthetic hydrological modelling approach the impact of climate change on drought occurrence and severity was studied. Drought characteristics; drought duration, standardized deficit volume and percentage of drought occurrence per year were calculated for the time period 1960–2100. Three different General Circulation

Models (ECHAM, CNRM, IPSL) were used as meteorological forcing to simulate possible effects of climate change on droughts (GCM forced models). The A2 emission scenarios was used to explore the most severe outcome for the three GCM forced models. Obtained drought characteristics were compared against the drought characteristics obtained from simulations of the hydrological model forced with meteorological data from the WATCH Forcing Data, which was used as a reference dataset in this study (reference model). Comparison was performed for the control period 1971–2000 and the deviations of each GCM forced model from the reference model were calculated. On a global scale drought duration found for the reference model and the GCM forced models were in the same order of magnitude, while the standardized deficit volume was underestimated compared against the reference model. It was concluded that the GCM forced models produce realistic meteorological forcing for future hydrological drought assessment, but have difficulties to capture the more extreme arid and polar climates.

The effects of climate change were studied for two period, namely 2021–2050 and 2071–2100 and compared relative to the control period. From the analysis it is concluded that average drought duration and standardized deficit volume will increase as a result of climate change. However, the total drought duration and number of droughts will decrease since on a global scale the total water availability will increase due to increased precipitation totals.

On a global scale the average duration of drought events will increase by a factor 1.5 in the far future (2071–2100), where this increase is most severe in the equatorial and arid climate types. Overall the total drought duration (PDY) decreases to 26–33 % relative to the control period, where the decrease is most striking in the snow climates. Increasing temperatures cause a decrease in winter droughts and snow accumulation, combined with increase precipitation leading to a very strong decrease in total drought duration (5–8 % relative to the control period). Global average drought standardized deficit volume increases by slightly more than 2 times for the period 2071–2100, which suggests that drought severity will increase as a result of changes in the climate.

Projections of global hydrological drought, which are essential for future water resources management, are still very limited. This study advances knowledge on future hydrological drought. Averaged over all climates the GCM forced hydrological models produces similar changes in drought in discharge. Some spread is found among the models, but the directionality is similar. In general, the synthetic hydrological modelling approach shows that hydrological drought occurrence (i.e. total days in drought per year) is projected to decrease over the 21st century, particularly in the temperate and cold climate regions. On the contrary, average drought duration and deficit volume of the remaining droughts are expected to substantially increase. The most critical impacts are projected for the already water scarce arid climates (B climates), where drought occurrence will not decrease that much and average duration and deficit volume of remaining drought events will increase more that in other climates. However, in this climate, model uncertainty is largest.

Acknowledgements. The authors would like to thank Graham Weedon (UK MetOffice) for supplying the WATCH Forcing Data. We appreciate very much the work done by Cui Chen, Jan Haerter and Stefan Hagemann (Terrestrial Hydrology Group, Max Planck Institute for Meteorology, Hamburg, Germany), Jens Heinke (Potsdam Institute for Climate Impact Research, Potsdam, Germany) and Claudio Piani (Abdus Salam International Centre for Theoretical Physics, Trieste, Italy) to downscale and bias correct the climate output from the three GCMs (daily data, 1960–2100) used in this study. This research has been financially supported by the EU-FP6 Project WATCH (contract 036946), the EU-FP7 Project DROUGHT-R&SPI (contract 282769) and NWO (NWO GO-AO/30). This research supports the work of the UNESCO-IHP VII FRIEND-Water programme.

References

Allen, R., Pereira, L., Raes, D., and Smith, M.: FAO Irrigation and Drainage Paper No. 56 – Crop Evapotranspiration, Food and Agriculture Organization, Rome, Italy, 2006. 7708

NHESSD
1, 7701–7738, 2013

Title Page
Abstract | Introduction
Conclusions | References
Tables | Figures
◀| |▶
◀ ▶
Back | Close
Full Screen / Esc
Printer-friendly Version
Interactive Discussion

Andreadis, K. M., Clark, E. A., Wood, A. W., Hamlet, A. F., and Lettenmaier, D. P.: Twentieth-century drought in the conterminous United States, J. Hydrometeorol., 6, 985–1001, doi:10.1175/JHM450.1, 2005. 7704

Arnell, N. W.: Effects of IPCC SRES* emissions scenarios on river runoff: a global perspective, Hydrol. Earth Syst. Sci., 7, 619–641, doi:10.5194/hess-7-619-2003, 2003. 7718, 7719

Chen, C., Haerter, J. O., Hagemann, S., and Piani, C.: On the contribution of statistical bias correction to the uncertainty in the projected hydrological cycle, Geophys. Res. Lett., 38, L20403, doi:10.1029/2011GL049318, 2011. 7707, 7714, 7718

Clyde, G.: Snow melting characteristics, Utah Agricultural Experiment Station bulletin, 231, 1–23, 1931. 7708

Collins, E. H.: Relationship of degree-days above freezing to runoff, transactions of the American Geophysical Union, reports and papers, Hydrology, 15, 624–629, 1934. 7708

Corzo-Perez, G. A., Van Lanen, H. A. J., Bertrand, N., Chen, C., Clark, D., Folwell, S., Gosling, S. N., Hanasaki, N., Heinke, J., and Voß, F.: Drought at the global scale in the 21st Century, Tech. Rep. 43, EU WATCH (Water and global Change) project, available at: www.eu-watch.org, last access: 1 March 2012, 2011. 7704, 7705, 7718, 7719

Dai, A.: Drought under global warming: a review, Climate Change, 2, 45–65, doi:10.1002/wcc.81, 2011. 7704

Dai, A.: Increasing drought under global warming in observations and models, Nature Climate Change, 3, 52–58, doi:10.1038/nclimate1633, 2012. 7717

Dai, A., Trenberth, K., and Qian, T.: A global dataset of Palmer Drought Severity Index for 1870–2002: relationship with soil moisture and effects of surface warming, J. Hydrometeorol., 5, 1117–1130, 2004. 7704

EEA: Mapping the impact of natural hazards and technological accidents in Europe. An overview of the last decade, Tech. Rep. 13/2010, EEA, Copenhagen, 2010. 7703

Feyen, L. and Dankers, R.: Impact of global warming on streamflow drought in Europe, J. Geophys. Res., 114, D17116, doi:10.1029/2008JD011438, 2009. 7718, 7719, 7720

Fichefet, T. and Maqueda, M. A. M.: Sensitivity of a global sea ice model to the treatment of ice thermodynamics and dynamics, J. Geophys. Res., 102, 12609–12646, doi:10.1029/97JC00480, 1997. 7706

Fleig, A. K., Tallaksen, L. M., Hisdal, H., and Demuth, S.: A global evaluation of streamflow drought characteristics, Hydrol. Earth Syst. Sci., 10, 535–552, doi:10.5194/hess-10-535-2006, 2006. 7710

NHESSD
1, 7701–7738, 2013

Future discharge drought

N. Wanders and H. A. J. van Lanen

Forzieri, G., Feyen, L., Rojas, R., Flörke, M., Wimmer, F., and Bianchi, A.: Ensemble projections of future streamflow droughts in Europe, Hydrol. Earth Syst. Sci. Discuss., 10, 10719–10774, doi:10.5194/hessd-10-10719-2013, 2013. 7704, 7718, 7719
Geiger, R.: Landolt-Börnstein – Zahlenwerte und Funktionen aus Physik, Chemie, Astronomie, Geophysik und Technik, alte Serie Vol. 3, Ch. Klassifikation der Klimate nach W. Köppen, Springer, Berlin, 603–607, 1954 (in German). 7713
Geiger, R.: Überarbeitete Neuausgabe von Geiger, R.: Köppen-Geiger/Klima der Erde, Wandkarte 1 : 16 Mill., Klett-Perthes, Gotha, 1961 (in German). 7713
Goosse, H. and Fichefet, T.: Importance of ice-ocean interactions for the global ocean circulation: a model study, J. Geophys. Res., 104, 23337–23355, doi:10.1029/1999JC900215, 1999. 7706
Gudmundsson, L., Tallaksen, L. M., Stahl, K., Clark, D. B., Dumont, E., Hagemann, S., Bertrand, N., Gerten, D., Heinke, J., Hanasaki, N., Voss, F., and Koirala, S.: Comparing large-scale hydrological model simulations to observed runoff percentiles in Europe, J. Hydrometeorol., 13, 604–620, doi:10.1175/JHM-D-11-083.1, 2011. 7703, 7704
Haddeland, I., Clark, D. B., Franssen, W., Ludwig, F., Voß, F., Arnell, N. W., Bertrand, N., Best, M., Folwell, S., Gerten, D., Gomes, S., Gosling, S. N., Hagemann, S., Hanasaki, N., Harding, R., Heinke, J., Kabat, P., Koirala, S., Oki, T., Polcher, J., Stacke, T., Viterbo, P., Weedon, G. P., and Yeh, P.: Multimodel estimate of the global terrestrial water balance: setup and first results, J. Hydrometeorol., 12, 869–884, doi:10.1175/2011JHM1324.1, 2011. 7703, 7704, 7718
Haerter, J. O., Hagemann, S., Moseley, C., and Piani, C.: Climate model bias correction and the role of timescales, Hydrol. Earth Syst. Sci., 15, 1065–1079, doi:10.5194/hess-15-1065-2011, 2011. 7707, 7714, 7718
Hagemann, S., Chen, C., Haerter, J. O., Heinke, J., Gerten, D., and Piani, C.: Impact of a statistical bias correction on the projected hydrological changes obtained from three GCMs and two hydrology models, J. Hydrometeorol., 12, 556–578, doi:10.1175/2011JHM1336.1, 2011. 7714, 7718
Hannah, D. M., Demuth, S., van Lanen, H. A. J., Looser, U., Prudhomme, C., Rees, G., Stahl, K., and Tallaksen, L. M.: Large-scale river flow archives: importance, current status and future needs, Hydrol. Process., 25, 1191–1200, doi:10.1002/hyp.7794, 2011. 7703

Hirabayashi, Y., Kanae, S., Emori, S., Oki, T., and Kimoto, M.: Global projections of changing risks of floods and droughts in a changing climate, Hydrolog. Sci. J., 53, 754–772, 2008. 7718

Hisdal, H., Tallaksen, L., Clausen, B., Peters, E., and Gustard, A.: Hydrological Drought Characteristics, in: Hydrological Drought: Processes and Estimation Methods for Streamflow and Groundwater, edited by: Tallaksen, L. and Lanen, H., no. 48 in Development in Water Science, 139–198, Elsevier, Amsterdam, The Netherlands, 2004. 7709

Hourdin, F., Musat, I., Bony, S., Braconnot, P., Codron, F., Dufresne, J.-L., Fairhead, L., Filiberti, M.-A., Friedlingstein, P., Grandpeix, J.-Y., Krinner, G., LeVan, P., Li, Z.-X., and Lott, F.: The LMDZ4 general circulation model: climate performance and sensitivity to parametrized physics with emphasis on tropical convection, Clim. Dynam., 27, 787–813, doi:10.1007/s00382-006-0158-0, 2006. 7706

Jungclaus, J. H., Keenlyside, N., Botzet, M., Haak, H., Luo, J.-J., Latif, M., Marotzke, J., Mikolajewicz, U., and Roeckner, E.: Ocean circulation and tropical variability in the coupled model ECHAM5/MPI-OM, J. Climate, 19, 3952–3972, doi:10.1175/JCLI3827.1, 2006. 7706

Köppen, W.: Versuch einer Klassifikation der Klimate, vorzugsweise nach ihren Beziehungen zur Pflanzenwelt., Geograf. Z., 6, 593–611, 657–679, 1900 (in German). 7713

Kraijenhof van de Leur, D.: Some effects of the unsaturated zone on nonsteady free-surface groundwater flow as studied in a sealed granular model, J. Geophys. Res., 67, 4347–4362, 1962. 7709

Madec, G., Delecluse, P., Imbard, M., and Lévey, C.: OPA version 8.1 Ocean General Circulation Model reference manual, University Paris VI, Paris, notes du pole de model, 11th Edn., 1998. 7706

McKee, T., Doesken, N., and Kleist, J.: The relationship of drought frequency and duration to time scales, in: Eighth Conference on Applied Climatology, 17–22 January, Anaheim, California, 1993. 7704

McMahon, T. A., Peel, M. C., Lowe, L., Srikanthan, R., and McVicar, T. R.: Estimating actual, potential, reference crop and pan evaporation using standard meteorological data: a pragmatic synthesis, Hydrol. Earth Syst. Sci., 17, 1331–1363, doi:10.5194/hess-17-1331-2013, 2013. 7708

Milly, P. C. D., Dunne, K. A., and Vecchia, A. V.: Global pattern of trends in streamflow and water availability in a changing climate, Nature, 438, 347–350, doi:10.1038/nature04312, 2005. 7718, 7719

NHESSD
1, 7701–7738, 2013

Future discharge drought

N. Wanders and H. A. J. van Lanen

Mishra, A. K. and Singh, V. P.: A review of drought concepts, J. Hydrol., 391, 202–216, doi:10.1016/j.jhydrol.2010.07.012, 2010. 7703

Mitchell, T. and Jones, P.: An improved method of constructing a database of monthly climate observations and associated high-resolution grids, Int. J. Climatol., 25, 693–712, 2005. 7706

Nakićenović, N., and Swart, R.: Special Report on Emissions Scenarios: A special report of Working Group III of the Intergovernmental Panel on Climate Change, Cambridge University Press, Cambridge, UK, 2000. 7706

National Oceanic and Atmospheric Administration, available at: www.ncdc.noaa.gov/sotc/drought/2012 (last access: 17 December 2012), 2012. 7703

Orlowsky, B. and Seneviratne, S. I.: Elusive drought: uncertainty in observed trends and short- and long-term CMIP5 projections, Hydrol. Earth Syst. Sci., 17, 1765–1781, doi:10.5194/hess-17-1765-2013, 2013. 7704, 7717

Palmer, W.: Meteorological drought, US Weather Bureau Research Paper, No. 45, 58 pp., Washington D.C, USA, 1965. 7704

Parry, S., Prudhomme, C., Hannaford, J., and Lloyd-Hughes, B.: Examining the spatio-temporal evolution and characteristics of large-scale European droughts, in: Role of Hydrology in Managing Consequences of a Changing Global Environment, Proceedings of the BHS Third International Symposium, edited by: Kirby, C., British Hydrological Society, Newcastle, UK, 135–142, 2010. 7710

Peters, E., Torfs, P., van Lanen, H., and Bier, G.: Propagation of drought through groundwater – a new approach using linear reservoir theory, Hydrol. Process., 17, 3023–3040, 2003. 7704

Piani, C., Haerter, J., and Coppola, E.: Statistical bias correction for daily precipitation in regional climate models over Europe, Theor. Appl. Climatol., 99, 187–192, doi:10.1007/s00704-009-0134-9, 2010a. 7707, 7714

Piani, C., Weedon, G., Best, M., Gomes, S., Viterbo, P., Hagemann, S., and Haerter, J.: Statistical bias correction of global simulated daily precipitation and temperature for the application of hydrological models, J. Hydrol., 395, 199–215, doi:10.1016/j.jhydrol.2010.10.024, 2010b. 7707, 7714

Prudhomme, C., Parry, S., Hannaford, J., Clark, D. B., Hagemann, S., and Voss, F.: How well do large-scale models reproduce regional hydrological extremes in Europe?, J. Hydrometeorol., 12, 1181–1204, doi:10.1175/2011JHM1387.1, 2011. 7703, 7704

NHESSD

1, 7701–7738, 2013

Future discharge drought

N. Wanders and H. A. J. van Lanen

Ritzema, H. (Ed.): Subsurface flow to drains, in: Drainage Principles and Applications, International Institute for Land Reclamation and Improvement, Wageningen, The Netherlands, 2nd Edn., 263–303, 1994. 7709

Roeckner, E., Bäuml, G., Bonaventura, L., Brokopf, R., Esch, M., Giorgetta, M., Hagemann, S., Kirchner, I., Kornblueh, L., Manzini, E., Rhodin, A., Schlese, U., Schulzweida, U., and Tompkins, A.: The atmospheric general circulation model ECHAM5 Part I, Tech. Rep. 349, Max-Planck-Institut für Meteorologie, Hamburg, Germany, 2003. 7706

Romm, J.: Desertification: the next dust bowl, Nature, 478, 450–451, doi:10.1038/478450a, 2011. 7703

Royer, J.-F., Cariolle, D., Chauvin, F., Déqué, M., Douville, H., Hu, R.-M., Planton, S., Rascol, A., Ricard, J.-L., Melia, D. S. Y., Sevault, F., Simon, P., Somot, S., Tyteca, S., Terray, L., and Valcke, S.: Simulation des changements climatiques au cours du XXIe siècle incluant l'ozone stratosphérique, Comptes Rendus Geoscience, 334, 147–154, doi:10.1016/S1631-0713(02)01728-5, 2002 (in French). 7706

Salas-Mélia, D.: A global coupled sea ice – ocean model, Ocean Model., 4, 137–172, doi:10.1016/S1463-5003(01)00015-4, 2002. 7706

Schneider, U., Fuchs, T., Meyer-Christoffer, A., and Rudolf, B.: Global precipitation analysis products of the GPCC, Global Precipitation Climatology Centre (GPCC), avaiable at: gpcc.dwd.de, last access: 15 February 2012, 2008. 7706

Seibert, J.: HBV Light Version 2 User's Manual, Stockholm University, Department of Physical Geography and Quaternary Geology, Stockholm, Sweden, 2002. 7708

Seneviratne, S. I., Nicholls, N., Easterling, D., Goodess, C. M., Kanae, S., Kossin, J., Luo, Y., Marengo, J., McInnes, K., Rahimi, M., Reichstein, M., Sorteberg, A., Vera, C., and Zhang, X.: Changes in climate extremes and their impacts on the natural physical environment, chap. A Special Report of Working Groups I and II of the Intergovernmental Panel on Climate Change (IPCC), Cambridge University Press, Cambridge, UK, and New York, NY, USA, 109–230, 2012. 7703, 7717

Sheffield, J. and Wood, E. F.: Drought: Past Problems and Future Scenarios, Earthscan, London, 2011. 7703

Sheffield, J. and Wood, F.: Characteristics of global and regional drought, 1950–2000: analysis of soil moisture data from off-line simulation of the terrestrial hydrologic cycle, J. Geophys. Res., 112, D17115, doi:10.1029/2006JD008288, 2007. 7704

Sheffield, J., Andreadis, K., Wood, E., and Lettenmaier, D.: Global and continental drought in the second half of the twentieth century: severity-Area-Duration analysis and temperol variability of large-scale events, J. Climate, 22, 1962–1981, 2009. 7704

Sheffield, J., Wood, E. F., and Roderick, M. L.: Little change in global drought over the past 60 years, Nature, 491, 435–438, doi:10.1038/nature11575, 2012. 7717

Solomon, S., Qin, D., Manning, M., Chen, Z., Marquis, M., Averyt, K., Tignor, M., and Miller, H.: Contribution of Working Group I to the Fourth Assessment Report of the Intergovernmental Panel on Climate Change, 2007, Tech. rep., IPCC, Cambridge, UK and New York, NY, USA, 2007. 7719

Sperna Weiland, F. C., van Beek, L. P. H., Kwadijk, J. C. J., and Bierkens, M. F. P.: The ability of a GCM-forced hydrological model to reproduce global discharge variability, Hydrol. Earth Syst. Sci., 14, 1595–1621, doi:10.5194/hess-14-1595-2010, 2010. 7718, 7719

Stahl, K., Tallaksen, L. M., Gudmundsson, L., and Christensen, J. H.: Streamflow data from small basins: a challenging test to high-resolution regional climate modeling, J. Hydrometeorol., 12, 900–912, doi:10.1175/2011JHM1356.1, 2011. 7717, 7720

Stahl, K., Tallaksen, L. M., Hannaford, J., and van Lanen, H. A. J.: Filling the white space on maps of European runoff trends: estimates from a multi-model ensemble, Hydrol. Earth Syst. Sci., 16, 2035–2047, doi:10.5194/hess-16-2035-2012, 2012. 7703, 7704

Tallaksen, L. and Van Lanen, H.: Hydrological Drought: Processes and Estimation Methods for Streamflow and Groundwater, no. 48 in Development in Water Science, Elsevier, Amsterdam, The Netherlands, 2004. 7703

Tallaksen, L., Madsen, H., and Clausen, B.: On the definition and modelling of streamflow drought duration and deficit volume, Hydrolog. Sci., 42, 15–33, 1997. 7709

Tallaksen, L., Hisdal, H., and van Lanen, H.: Space-time modelling of catchment scale drought characteristics, J. Hydrol., 375, 363–372, 2009. 7704

Tijdeman, E., Van Loon, A. F., Wanders, N., and Van Lanen, H. A. J.: The effect of climate on droughts and their propagation in different parts of the hydrological cycle, Tech. Rep. 2, EU-Drought-R-SPI, Wageningen, The Netherlands, 2012. 7709

United Nations: Humanitarian requirements for the Horn of Africa drought 2011, Tech. rep., Office for the Coordination of Humanitarian Affairs (OCHA), New York and Geneva., 2011. 7703

Uppala, S. M., Kallberg, P. W., Simmons, A. J., Andrae, U., Bechtold, V. D. C., Fiorino, M., Gibson, J. K., Haseler, J., Hernandez, A., Kelly, G. A., Li, X., Onogi, K., Saarinen, S., Sokka, N., Allan, R. P., Andersson, E., Arpe, K., Balmaseda, M. A., Beljaars, A. C. M., Berg, L. V. D., Bidlot, J., Bormann, N., Caires, S., Chevallier, F., Dethof, A., Dragosavac, M., Fisher, M., Fuentes, M., Hagemann, S., Hólm, E., Hoskins, B. J., Isaksen, L., Janssen, P. A. E. M., Jenne, R., McNally, A. P., Mahfouf, J. F., Morcrette, J. J., Rayner, N. A., Saunders, R. W., Simon, P., Sterl, A., Trenberth, K. E., Untch, A., Vasiljevic, D., Viterbo, P., and Woollen, J.: The ERA-40 re-analysis, Q. J. Roy. Meteor. Soc., 131, 2961–3012, 2005. 7706

van Huijgevoort, M. H. J., Hazenberg, P., van Lanen, H. A. J., and Uijlenhoet, R.: A generic method for hydrological drought identification across different climate regions, Hydrol. Earth Syst. Sci., 16, 2437–2451, doi:10.5194/hess-16-2437-2012, 2012. 7704

Van Lanen, H., M., F., Kupczyk, E., Kasprzyk, A., and Pokojski, W.: Flow generating processes, in: Hydrological Drought: Processes and Estimation Methods for Streamflow and Groundwater, edited by: Tallaksen, L. and van Lanen, H., no. 48 in Development in water science, Elsevier, Amsterdam, The Netherlands, 53–98, 2004.

Van Lanen, H. A. J., Wanders, N., Tallaksen, L. M., and Van Loon, A. F.: Hydrological drought across the world: impact of climate and physical catchment structure, Hydrol. Earth Syst. Sci., 17, 1715–1732, doi:10.5194/hess-17-1715-2013, 2013. 7717
7705, 7709, 7712, 7713

Van Loon, A. F. and Van Lanen, H. A. J.: A process-based typology of hydrological drought, Hydrol. Earth Syst. Sci., 16, 1915–1946, doi:10.5194/hess-16-1915-2012, 2012. 7703, 7704, 7710, 7720

Van Loon, A. F., Van Huijgevoort, M. H. J., and Van Lanen, H. A. J.: Evaluation of drought propagation in an ensemble mean of large-scale hydrological models, Hydrol. Earth Syst. Sci., 16, 4057–4078, doi:10.5194/hess-16-4057-2012, 2012. 7717

Van Vliet, M. T. H., Yearsley, J. R., Ludwig, F., Vogele, S., Lettenmaier, D. P., and Kabat, P.: Vulnerability of US and European electricity supply to climate change, Nature Clim. Change, 2, 676–681, doi:10.1038/nclimate1546, 2012. 7703

Wand, M. P. and Jones, M. C.: Kernel Smoothing, Chapman and Hall, London, 1995. 7712

Wanders, N., Van Lanen, H. A. J., and Van Loon, A. F.: Indicators for drought characterization on a global scale., Tech. Rep. 24, EU-WATCH, Wageningen, The Netherlands, 2010. 7713

Weedon, G., Gomes, S., Viterbo, P., Österle, H., Adam, J., Bellouin, N., Boucher, O., and Best, M.: The WATCH Forcing Data 1958–2001: a meteorological forcing dataset for land

surface- and hydrological models., Tech. Rep. 22, EU WATCH (Water and global Change) project, Wallingford, UK, 2010. 7706
Weedon, G. P., Gomes, S., Viterbo, P., Shuttleworth, W. J., Blyth, E., Österle, H., Adam, J. C., Bellouin, N., Boucher, O., and Best, M.: Creation of the WATCH forcing data and its use to assess global and regional reference crop evaporation over land during the twentieth century, J. Hydrometeorol., 12, 823–848, doi:10.1175/2011JHM1369.1, 2011. 7706
Wilhite, D.: Drought: A global assessment, London, UK, 2000. 7703
Wilson, D., Hisdal, H., and Lawrence, D.: Has streamflow changed in the Nordic countries? – Recent trends and comparisons to hydrological projections, J. Hydrol., 394, 334–346, doi:10.1016/j.jhydrol.2010.09.010, 2010. 7720
Wong, W. K., Beldring, S., Engen-Skaugen, T., Haddeland, I., and Hisdal, H.: Climate change effects on spatiotemporal patterns of hydroclimatological summer droughts in Norway, J. Hydrometeorol., 12, 1205–1220, doi:10.1175/2011JHM1357.1, 2011. 7720
Yevjevich, V.: An Objective Approach to Definition and Investigation of Continental Hydrological Droughts, Hydrology papers, 23, Colorado state university, Fort Collins, USA, 1967. 7709

NHESSD
1, 7701–7738, 2013

Future discharge drought

N. Wanders and H. A. J. van Lanen

Table 1. Three IPCC AR4 GCMs an their properties.

Centre	GCM	Horizontal res.	Vertical res.
MPI	ECHAM5/MPIOM T63	$\approx 1.9^{\circ} \approx 200$ km	31 Layers
CNRM	CNRM-CM3 T42	$\approx 2.8^{\circ} \approx 300$ km	45 Layers
IPSL	IPSL-CM4	$3.75^{\circ} \times 2.5^{\circ} \approx 300$ km	19 Layers

NHESSD
1, 7701–7738, 2013

Table 2. Similarity Index (SI) between the reference model with meteorological forcing from the WATCH Forcing Data and models with meteorological forcing from three General Circulation Models (ECHAM, CNRM, IPSL) for the control period (1971–2000). SI is given for all major climates, Equatorial (A), Arid (B), Warm temperate (C), Snow (D) and Polar climates (E) and averaged over all climates.

	WFD					
	A	B	C	D	E	All
ECHAM	100	75	99	92	67	91
CNRM	100	82	100	87	73	94
IPSL	100	85	98	90	65	93

NHESSD
1, 7701–7738, 2013

Future discharge drought

N. Wanders and H. A. J. van Lanen

Table 3. Average drought characteristics for the control period (1971–2000), including % relative to the WATCH Forcing Data. Characteristics are provided for Equatorial (A), Arid (B), Warm temperate (C), Snow (D) and Polar climates (E).

		WFD	ECHAM	CNRM	IPSL
Duration (d)	A	54.3	57.3 (106 %)	59.5 (110 %)	70.7 (130 %)
	B	79.4	57.4 (72 %)	63.1 (79 %)	66.5 (84 %)
	C	50.2	49.3 (98 %)	54.6 (109 %)	51.4 (102 %)
	D	57.1	56.5 (99 %)	57.0 (100 %)	55.5 (97 %)
	E	105.0	48.8 (46 %)	51.8 (49 %)	47.2 (45 %)
	All	66.7	59.8 (90 %)	69.0 (103 %)	66.6 (100 %)
Standardized deficit volume (d)	A	5.31	4.58 (86 %)	5.25 (99 %)	6.61 (124 %)
	B	8.44	4.89 (58 %)	5.85 (69 %)	5.47 (65 %)
	C	4.73	4.26 (90 %)	5.01 (106 %)	4.13 (87 %)
	D	5.61	4.82 (86 %)	4.43 (79 %)	4.14 (74 %)
	E	10.89	4.08 (37 %)	4.24 (39 %)	3.64 (33 %)
	All	6.58	5.05 (77 %)	5.94 (90 %)	5.24 (80 %)

NHESSD
1, 7701–7738, 2013

Future discharge drought

N. Wanders and
H. A. J. van Lanen

Table 4. Changes in median of drought characteristics (% relative to control period, 1971–2000) for climate types: Equatorial (A), Arid (B), Warm temperate (C), Snow (D) and Polar climates (E).

		2021–2050			2071–2100		
		ECHAM	CNRM	IPSL	ECHAM	CNRM	IPSL
Duration (d)	A	142	138	131	175	169	181
	B	142	133	144	175	160	181
	C	133	123	115	150	162	162
	D	107	93	100	129	121	114
	E	100	108	108	123	138	131
	All	115	114	121	146	143	157
PDY ($d\,yr^{-1}$)	A	81	75	112	74	44	128
	B	95	81	98	89	56	99
	C	78	65	49	41	40	22
	D	57	49	47	8	5	8
	E	61	53	52	22	19	25
	All	70	61	62	33	26	30
Standardized deficit volume (d)	A	193	194	182	301	317	327
	B	206	179	218	305	268	310
	C	164	145	134	217	220	247
	D	131	103	117	144	152	126
	E	115	128	115	147	170	167
	All	155	139	146	206	214	222

NHESSD
1, 7701–7738, 2013

N. Wanders and H. A. J. van Lanen

Table 5. Similarity Index (SI) for the near (2021–2050) and far (2071–2100) future, compared to the control period (1971–2000) derived from a hydrological model forced with three General Circulation Models. SI is given for all major climates, Equatorial (A), Arid (B), Warm temperate (C), Snow (D) and Polar climates (E) and averaged over all climates.

	Control period					
	A	B	C	D	E	All
ECHAM 2021–2050	77	71	73	84	84	81
ECHAM 2071–2100	63	60	64	70	73	69
CNRM 2021–2050	78	82	85	88	81	87
CNRM 2071–2100	64	71	68	64	68	71
IPSL 2021–2050	73	71	83	87	86	82
IPSL 2071–2100	60	58	63	73	71	68

NHESSD
1, 7701–7738, 2013

N. Wanders and
H. A. J. van Lanen

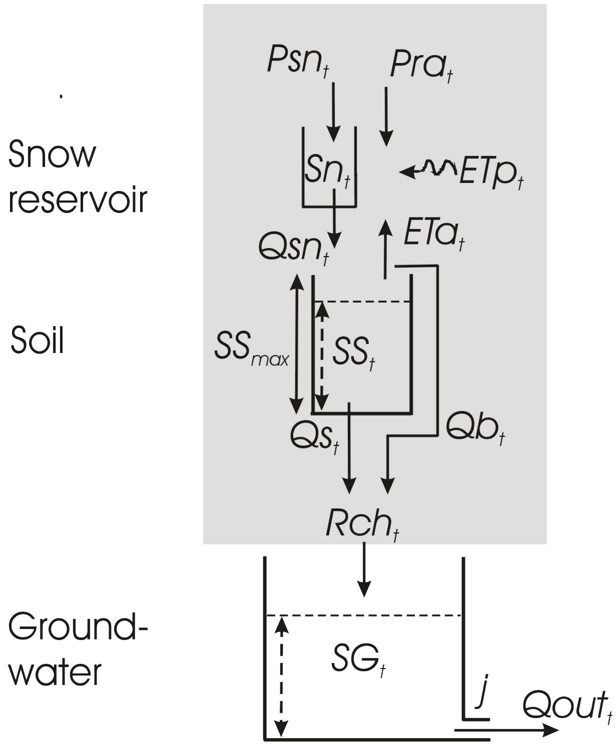

Fig. 1. Model set-up.

NHESSD
1, 7701–7738, 2013

N. Wanders and
H. A. J. van Lanen

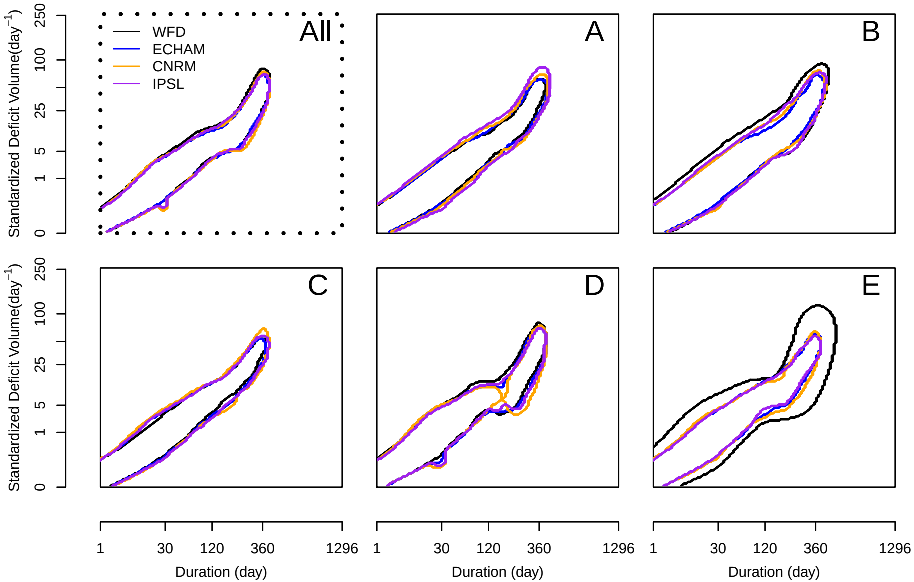

Fig. 2. Bivariate probability functions for two drought characteristics (duration and standardized deficit volume) for all climate types **(All)** and individual major climate types, Equatorial **(A)**, Arid **(B)**, Warm temperate **(C)**, Snow **(D)** and Polar climates **(E)** obtained from hydrological models using meteorological forcing by the WATCH Forcing Data (WFD) and General Circulation Models; ECHAM, CNRM and IPSL.

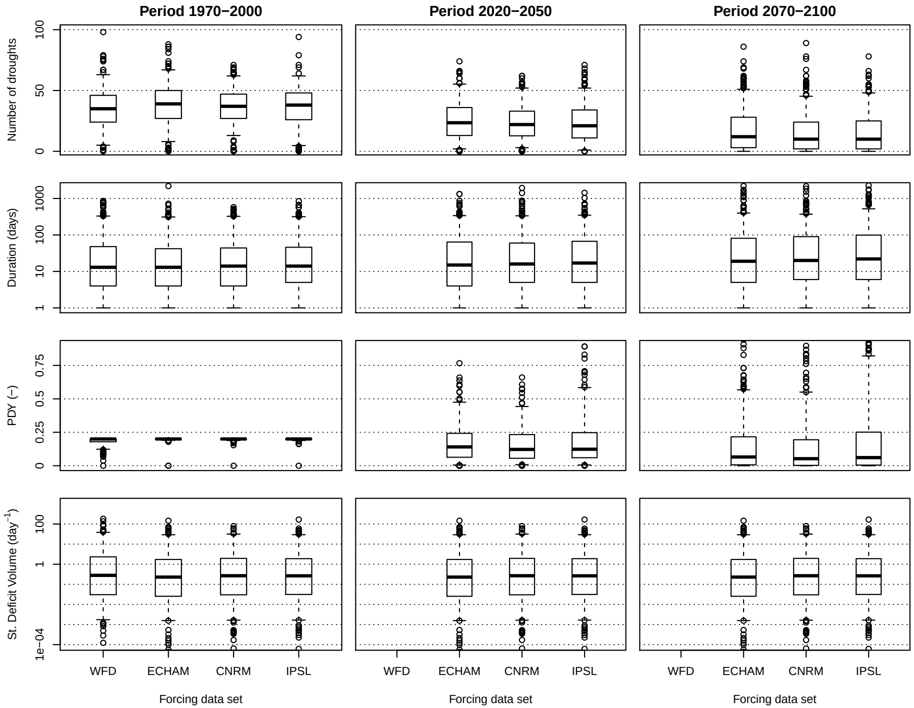

Fig. 3. Distribution of three discharge drought characteristics obtained from a hydrological model using meteorological forcing from the WATCH Forcing Data (reference model) and three models with meteorological forcing from General Circulation Models (ECHAM, CNRM and IPSL) for the control period (1971–2000). Row one indicates the number of droughts per evaluation period, row two the average drought duration, row three the percentage of the year in drought and the last row gives the average standardized deficit volume.

NHESSD
1, 7701–7738, 2013

Future discharge drought

N. Wanders and H. A. J. van Lanen